



Improved model predictions of carbon and water fluxes by including drought legacy effects

Yitong Yao^{1,*}, Yujie Wang^{1,*}, Yi Yin¹, Jeffrey D. Wood², Christian Frankenberg^{1,3}

- ¹ 1 Division of Geological and Planetary Sciences, California Institute of Technology, Pasadena, CA 91125, USA
- 2 School of Natural Resources, University of Missouri, Columbia, MO 65211, US
- 3 Jet Propulsion Laboratory, California Institute of Technology, Pasadena, CA 91109, USA

Correspondence to: Yitong Yao (yyao2@caltech.edu) and Yujie Wang (wyujie@ustc.edu.cn)

Abstract. Besides simultaneous influences, droughts have lasting impacts on vegetation by impairing hydraulic and photosynthetic capacities, known as the drought legacy effects. The ignorance of legacy effects in numerical simulations, such as lagged xylem recovery, may lead to significant model-observation discrepancies. However, the limited temporal resolution of most observational data makes it challenging to capture the physiological dynamics necessary to improve model accuracy. Here, we investigated the recovery of carbon flux (represented by gross primary productivity, GPP) and water flux (represented by evapotranspiration, ET) following a severe drought in 2012, using half-hourly eddy-covariance flux observations and weekly predawn leaf water potential measurements from a temperate forest in the Central US. We implemented both optimality-based and empirical stomatal models within a land surface model, testing three drought recovery scenarios for each: no recovery, full recovery, and partial recovery of xylem hydraulic conductance and photosynthetic capacity. Before and during the drought, all stomatal models performed similarly for GPP and ET. Postdrought, assuming no recovery led to underestimated ET; assuming full recovery led to overestimated GPP; and assuming partial recovery improved both, indicating persistent biochemical limitations after drought. The observed carbon-water decoupling during and after the event further points to non-stomatal constraints on photosynthesis and unequal stress on carbon and water fluxes. Our work highlights the need to account for delayed recovery of xylem hydraulics and photosynthetic capacity when modeling drought legacy effects. Further research to mechanistically represent dynamic recovery processes, particularly their timing and magnitude, is essential for improving the modeling of global carbon and water fluxes.

25 1 Introduction

Plants are exposed to increasing frequency and severity of extreme events under climate change, such as heatwaves and droughts (Piao et al., 2019; Xu et al., 2019). During droughts, reduced precipitation and higher evaporation demand driven by rising air temperature usually lead to further depletion of soil moisture (Bastos et al., 2020; Wolf et al., 2016). Although plants partially close their stomata to protect their hydraulic systems from excessive damage (Sperry et al., 2017; Wang et al., 2020), they often suffer irreversible hydraulic impairment due to xylem cavitation. As a result, even after meteorological drought conditions are alleviated, persistent hydraulic damage limits water transport to leaves and a





downregulation of photosynthesis capacity may persist (Müller and Bahn, 2022). The reduced photosynthetic capacity during and after drought conditions, caused by insufficient water supply, further delays recovery to pre-drought functionality. This lagged recovery, often referred to as the drought legacy effect, can shift ecosystems from carbon sinks to carbon sources and increase plant mortality (Ciais et al., 2005). Vegetation models, however, often fail to accurately capture drought responses and legacy effects (Anderegg et al., 2015), as they typically oversimplify plant hydraulic processes and stomatal behavior, neglecting the persistent damage to hydraulic and photosynthetic systems. Quantifying the magnitude and timing of hydraulic impairment and recovery is therefore essential particularly for local scale modeling and important also for large-scale land surface and Earth system models to better represent the global carbon cycle.

40

Typical model simulations simplify the complexity and diversity of ecosystems by using plant functional type (PFT)-specific parameters to represent ecosystem responses. These models are often constrained by ecosystem-level measurements, which reflect the average of potentially divergent responses within the system. To simulate the effects of drought on CO₂ assimilation and transpiration loss, models often use a scaling factor (β) ranging from 0 to 1, to attenuate photosynthesis and/or stomatal conductance. Empirical stomatal models like the Ball-Berry model (Ball et al., 1987), Medlyn model (Medlyn et al., 2011), and Leuning model (Leuning, 1995), typically include a semi-empirical stomatal slope parameter g1, which reflects the efficiency of carbon gain relative to water cost. The accuracy of these models largely depends on the representation of water stress impacts on photosynthesis. Drought responses in photosynthesis are driven by both stomatal and non-stomatal limitations as shown through observations and model studies (Drake et al., 2017; Egea et al., 2011). However, the relative importance of these two components varies across studies (Gourlez de la Motte et al., 2020; Keenan et al., 2009, 2010; Reichstein et al., 2003; Zhou et al., 2015, 2013), and depends on the intensity and duration of water stress (Niinemets and Keenan, 2014). These limitations can be incorporated into models by either reducing the well-watered maximum carboxylation rate (Vcmax) to account for biochemical constraints (Kennedy et al., 2019) or adjusting the stomatal slope parameter (g1) to represent biophysical limitations (De Kauwe et al., 2015).

55

After drought events, the scaling factor β is often assumed to return to 1 as soil water refills (Fang and Gentine, 2024). Many terrestrial ecosystem models presume that this recovery is both immediate and complete, leading to the full restoration of carboxylation efficiency, stomatal conductance, and associated carbon and water fluxes. However, this assumption is likely invalid, as many studies have documented persistent drought legacy effects lasting from subseasonal to multi-year time scales (Anderegg et al., 2015; Kannenberg et al., 2020; Wu et al., 2018). These effects have been observed through carbon flux measurements (Yu et al., 2022), tree ring width analysis (Anderegg et al., 2015), and vegetation greenness indices (Wu et al., 2018) using both field observations and satellite data. This evidence highlights a critical limitation in the full recovery assumption commonly employed in models. Despite advancements in our understanding of plant physiological responses to drought, there remains a substantial knowledge gap regarding the key factors driving drought legacy effects and their underlying mechanisms. Addressing this gap is essential for improving the accuracy of ecosystem models in representing post-drought recovery processes.

70 c iii

75

65

A potential explanation for drought legacy effects is the incomplete recovery of hydraulic conductance, even after soil moisture has refilled, which limits upward water transport to the canopy (Kannenberg et al., 2020). This residual stress can propagate into biochemistry (Vcmax) and impose limitations on intrinsic water use efficiency through g1. However, the incomplete recovery of hydraulic conductance, Vcmax, or g1 has not been explicitly incorporated into most process-based models. Traditionally, water stress in models is represented as a nonlinear function of soil moisture content. Recent advancements in modeling the soil-plant-atmosphere continuum have improved the representation of plant water stress (Eller et al., 2020; Kennedy et al., 2019; Wang et al., 2021; Xu et al., 2016; Yao et al., 2022). These advancements incorporate vertically-resolved water pressure profiles and hydraulic traits through vulnerability curves, enabling the simulation of





dynamic hydraulic conductance over time. In this context, imposing limits on hydraulic conductance offers a practical way to represent the incomplete recovery of hydraulic function after soil moisture refilling. These limits reflect the 'stress history' experienced by plants, which can be inferred from observational data. Although drought legacy effects have been observed across a variety of metrics and time scales (Anderegg et al., 2015; Yu et al., 2022), higher temporal resolution data often provides better opportunities for model-data assimilation compared to coarser datasets. By integrating high-resolution observational carbon and water flux data with improved modeling frameworks, we can better understand the dominant controls on ecosystem-level drought legacy effects and their long-term impacts on ecosystem functioning.

In the summer of 2012, the Central US experienced a severe drought that rapidly developed and intensified over less than two months (Basara et al., 2019). This study focuses on the Missouri Ozark AmeriFlux (MOFLUX) eddy-covariance site located at the epicenter of the drought, providing an ideal setting to investigate drought effects. Using a land surface model (Climate Modeling Alliance, CliMA, (Wang et al., 2021)) and flux observations from the MOFLUX site, we aim to test the model's performance by incorporating drought legacy effects assimilated from observations. Our study was driven by three main objectives:

- (1) simulating the drought response using the CliMA land surface model.
- (2) identifying the relative strength of biochemical and stomatal factors in limiting carbon and water fluxes after the drought.
 - (3) diagnostically integrating legacy effects to test model performance under different recovery scenarios.

To assess the generalizability of the modeling framework, we extended the analysis by conducting simulations for five additional sites affected by the 2012 drought. The findings of our research will contribute to a better understanding of recovery processes and the factors driving drought legacy effects, enabling more accurate identification of where and how to apply stress factors in models.

2 Materials and methods

2.1 US-MOz site

90

100

105

110

115

The MOFLUX eddy-covariance flux tower (AmeriFlux ID: US-MOz) is located in the Central US (latitude: 38.7441, longitude: -92.2000), and characterized by a warm, humid and continental climate zone. The mean annual temperature is 13 °C and the mean annual precipitation is 1,140 mm. Important tree species in the area are white oak (*Quercus alba*), black oak (*Q. velutina*), sugar maple (*Acer saccharum*), shagbark hickory (*Carya ovata*), and eastern redcedar (*Juniperus virginiana*) (Gu et al., 2015). We used half-hourly measurements of evapotranspiration (ET), as well as net ecosystem carbon dioxide exchange (NEE) from which gross primary productivity (GPP) was inferred using the night-time partitioning method. The processing of carbon and water fluxes data used here follows the standardized AmeriFlux pipelines (Gu et al., 2016). Site-level leaf area index (LAI) was extracted using the GriddingMachine package (Wang et al., 2022) from MODIS (MODerate resolution Imaging Spectroradiometer) LAI products (Yuan et al., 2011). Predawn leaf water potential (Ψ_{leaf,pd}) measurements were initiated in 2004 and were carried out weekly to bi-weekly.

The 2012 drought is one of the most extensive drought events over the Central US on record, with rapid development and pronounced area encompassed by persistent dryness and warm temperatures. Specifically, nearly 64% of the area was characterized as 'at least moderate drought' in July as a peak. Wood et al. (Wood et al., 2023) divided the 2012 growing season into four stages: peak flux (DOY 125-150), flash stress (DOY 160-180), wilted (DOY 185-240), and recovery (DOY 255-270). We slightly modified these period definitions to eliminate any gaps between them, defining the stages as follows: peak flux (DOY 125 - 150), flash stress (DOY 150 - 180), wilted (DOY 180 - 240), and recovery (DOY 240 - 280).





2.2 Vegetation module of CliMA Land

We used the vegetation module of the land surface model developed within the Climate Modeling Alliance (CliMA) (Wang et al., 2021, 2023). The model's performance has been validated in terms of carbon and water fluxes, as well as solar-induced chlorophyll fluorescence (Braghiere et al., 2021; Wang et al., 2021, 2023). The model is highly modularized, including two radiative transfer schemes (broadband or hyperspectral), three photosynthesis models (two C3 models and one C4 model), eight stomatal models (empirical or optimality-based), and customization of the hydraulic system.

125

130

120

We ran CliMA Land in hyperspectral mode for radiative transfer and with a vertically resolved canopy, each layer of which was further split into sunlit and shaded fractions based on uniform leaf inclination and azimuthal distributions (Wang and Frankenberg, 2022; Zhao et al., 2019). The physiological parameters governing photosynthetic traits remain constant throughout the canopy. However, as the model separately accounts for the light environment of leaves across different layers, leaves can have distinct stomatal conductance, resulting in varying photosynthetic rates. At each time step, the fraction of sunlit leaf and absorbed photosynthetically active radiation (APAR) are calculated. For different stomatal models, with the steady-state stomatal conductance for each APAR value, we computed the corresponding leaf net photosynthetic rate using the classic C3 photosynthesis model (Farquhar et al., 1980). Finally, the canopy carbon and water fluxes are summed up over the entire canopy. The CliMA Land model incorporates changes in phenology by using 8-day LAI data from the MODIS product as input. The daily LAI value is then distributed across different canopy layers, thereby influencing carbon and water fluxes integrated from the entire canopy. For example, the whole canopy net photosynthesis is computed as:

$$\frac{LAI}{n_{canopy}} \left\{ \sum_{\substack{n_{azim}, n_{incl}, n_{canopy} \\ n_{azim}, n_{incl}, n_{canopy}}} \left[A_{net} P_{azim, incl, n} \right] + \sum_{n} A_{net} P_{shade, n} \right\}$$

Pazim.incl,n: fraction of the sunlit part for each bin of azimuth angle and inclination angle combination.

140 P_{shade,n}: fraction of the shaded part in the nth layer.

n_{canopy}: number of canopy layers. In this study, n_{canopy}=19.

n_{azim}: number of azimuth angle bins. In this study, n_{azim}=36.

n_{incl}: number of inclination angle bins. In this study, n_{incl}=9.

A_{net}: net carbon assimilation of one bin of azimuth angle and inclination angle.

145 LAI: 8-day LAI from MODIS products. A linear interpolation is used to obtain daily LAI values.

Carbon uptake response is influenced by both canopy structure and plant physiology, with our study focusing more on the biochemical and biophysical aspects. Canopy structure, representing phenology, has been accounted for by incorporating LAI variations, including reductions during wilted periods due to leaf shedding (Figure S1).

150

To demonstrate the model's capability in simulating canopy spectra, we compared the modeled NDVI with MODIS products. Using Google Earth Engine, we extracted the 2012 NDVI time series from the MOD09GA v006 product, which provides daily surface reflectance data. A maximum value composite method was applied to obtain monthly NDVI values. All variables were standardized based on the mean and standard deviation of seasonal values during the growing season. Our model effectively captured the observed seasonal variations in NDVI (Figure S2).

155

Here, we configured CliMA Land to use two stomatal models (Medlyn et al., 2011; Wang et al., 2021), and a hydraulic system with 2 root layers and 19 canopy layers. Each root layer represents a horizontal soil layer and includes two components arranged in series: the rhizosphere and the root xylem, with water flowing sequentially through both. All root



165

175



layers are connected in parallel to the base of the trunk. Root hydraulic resistance contributes to the overall plant hydraulic conductance, with a fixed root:stem:leaf resistance ratio of 2:1:1, consistent with the values used by Sperry et al. (Sperry et al., 2017). Specifically, we used a water stress factor (β), the ratio between the whole-plant hydraulic conductance primarily affected by the leaf water potential and the maximum hydraulic conductance, the former of which has been vertically resolved along the soil-plant-atmosphere continuum. Wood capacitance and water storage dynamics were not included. Soil respiration is modeled using the Arrhenius equation with parameterized temperature sensitivity of soil respiration. Here the model does not simulate soil evaporation and re-evaporation of rainfall interception, so we used a fixed T/ET ratio (0.67, falling in range reported in Fatichi and Pappas (Fatichi and Pappas, 2017)) to link the modeled plant transpiration to ET observation. Changing this T/ET ratio does not impact our results. The CliMA Land model was employed to reproduce the dynamics of carbon and water fluxes during the drought period.

170 2.3 Stomatal conductance models

The CliMA Land model incorporates several stomatal optimality models and three empirical stomatal models: the Medlyn, Ball-Berry and Leuning models. In this study, we used the Medlyn stomatal model and an optimality stomatal model designed to maximize the difference between carbon gains and the risks associated with leaf hydraulic failure and reduced photosynthesis (Wang et al., 2021). Empirical models can be effectively combined with two main categories of tuning factors to induce a stomatal response to drought. The first category operates by adjusting parameters of the empirical stomatal models, such as the slope parameter (g1). The second category involves the modulation of photosynthetic capacity through down-regulation, which also reduces stomatal conductance in drought conditions, as photosynthesis is reduced. When evaluating stomatal models, stress was either imposed 'directly' to the g1 parameter or 'indirectly' by modifying Vcmax, accounting for non-biochemical or biochemical limitations, respectively (Table 1).

80 **Table 1.** Stomatal models used in this study. C_s is the CO_2 concentration at the leaf surface. Γ is the canopy CO_2 compensation point.

Model	β on g1	β on Vcmax
Medlyn model	$g_s = g_0 + \beta \times (1 + \frac{g_1}{\sqrt{VPD}}) \times \frac{A_n}{C_s}$	$g_s = g_0 + (1 + \frac{g_1}{\sqrt{VPD}}) \times \frac{A_n(\beta)}{C_s}$

2.4 Hydraulic conductance recovery scenarios

As the leaf water potential becomes more negative due to lower soil water supply or higher atmospheric water demand, hydraulic conductance decreases, and xylem embolism could be triggered. Xylem functioning determines whether the rewatering can lead to an increase of water potential and recovery of hydraulic conductance. Three scenarios are considered regarding the recovery of hydraulic conductance after the occurrence of severe water stress conditions. For each stomatal conductance model (Section 2.3), these three recovery scenarios are applied (Table 2).

• Full recovery scenario (FR): Leaf water potential is prognostically updated. The vulnerability curve is prescribed from Benson et al. (Benson et al., 2022). The hydraulic conductance can either increase or decrease and the shape of the vulnerability curve remains constant, i.e. is not affected by the previous severe water stress condition. In other words, the water potential and hydraulic conductance can be updated without specific boundaries. Only transient (or immediate) responses are considered.





- Partial recovery scenario (PR): In reality, the full recovery of the hydraulic system may not necessarily occur due to irreversible processes such as a broken hydraulic transport system (e.g., embolism). Recovery can vary depending on the time scale; for instance, the construction of new xylem over time may facilitate greater recovery, while immediate recovery following a drought may be limited. The extent of potential plant recovery can be inferred from the response of carbon and water fluxes to post-drought climate conditions by applying a similar concept with optimizing ecosystem models through assimilating eddy-covariance measurements in Wolf et al. (Wolf et al., 2006). If this 'full recovery' assumption leads to overestimation of carbon and/or water fluxes, legacy effects can be inferred from the resulting bias relative to observations. By minimizing the difference between modeled and observed carbon and water fluxes, we diagnostically derived the water stress time series and updated modeled leaf water potential at each time step, as the water stress indicator is directly linked to the magnitude of leaf water potential in the model. The extent of hydraulic conductance recovery is estimated from newly-calculated percentage loss of hydraulic conductance (PLC) from diagnostic water potential series.
- No recovery scenario (NR): Hydraulic conductance can't increase (recover) over time. During severe water stress events, hydraulic conductance decreases due to a drop in water potential. Subsequently, during the post-drought period, hydraulic conductance cannot increase or return to its pre-drought state.

Correspondingly, assuming complete recovery of hydraulic conductance, the model simulation provides a post-drought estimation of the 'normal level'. Any deviation from this 'normal level' estimate reflects the legacy effect size based on observations. Subsequently, drawing on a similar concept of optimizing ecosystem models through assimilating eddy-covariance flux measurements (Wolf et al., 2006), a water stress series, indicative of legacy effects due to compromised hydraulic conductance, can be inverted and constrained by observed carbon and water fluxes, leading to a better understanding of the dominant control on ecosystem-level lagged responses.

Table 2. Model simulations for 9 scenarios, combining full, partial, or no recovery assumptions with three stomatal conductance models separately. Medlyn-Vcmax refers to applying the β factor to Vcmax, while Medlyn-g1 refers to applying the β factor to g1.

	Optimality (Opt)	Medlyn-Vcmax	Medlyn-g1
Full recovery	✓	✓	✓
Partial recovery	✓	✓	✓
No recovery	✓	✓	✓

2.5 Model parameters

220

225

We utilized vegetation traits such as the vulnerability curve, Vcmax at 25 °C, semi-empirical slope parameter (g1) that characterizes the efficiency of carbon gain relative to water cost, and maximum hydraulic conductance (K_{max}), using parameters from published references wherever possible. The well-watered Vcmax value was obtained from A/Ci curves measurements made at the site in May 2012, when the plants had not been hit by the severe water stress and $\Psi_{leaf,pd}$ was close to 0 MPa (Gu et al., 2010). We took the average of the Vcmax derived from these measurements (65.8 ±18.8 μ mol m⁻² s⁻¹). We used the 'fitaci' function in package 'plantecophys' version 1.4-6 (Duursma, 2015) to derive the fitted Vcmax at 25 °C. The root mean squared error from fitting is between 0.48-2.68 μ mol m⁻² s⁻¹. We used g1 value for deciduous broadleaf forests from De Kauwe et al. (De Kauwe et al., 2015). For the vulnerability curve (VC) of white oak, we used the sigmoid format parameters from Benson et al. (Benson et al., 2022) and transformed it to Weibull function format, which better fits the observations. The vulnerability curve was used to compute the stress factor β (Eq. 1). Ψ 63 indicates the xylem pressure at





~63% loss of conductivity, and b is the shape parameter (Neufeld et al., 1992). This β formula is the same for stomatal and non-stomatal limitations. We did not find measurements for K_{max}, therefore, this parameter was fitted by minimizing the error of ET between the model simulations and eddy-covariance observations over the pre-recovery periods (Eq. 2). Different K_{max} values were obtained depending on the chosen stomatal models, the location of the water stress factor, and recovery assumptions (Table S1). We also optimized K_{max} over longer pre-drought periods, extending to earlier years, which revealed notable inter-annual variability. For instance, in years with less water stress, such as 2010, the optimized K_{max} was significantly higher (2.81 mol m⁻² s⁻¹ MPa⁻¹) compared to 2012, a drought year (0.89 mol m⁻² s⁻¹ MPa⁻¹). This discrepancy suggests that the K_{max} derived from pre-drought periods may not fully capture potential hydraulic conductance damage. Consequently, we optimized K_{max} using 2012 data alone.

$$\beta = e^{-\left(-\frac{\varphi}{\varphi 63}\right)^b}$$
 Eq. (1)

240 where Ψ 63=2.94, b=2.52

245

265

For
$$K_{max}$$
: error function = $\sum \frac{|ET_{mod} - ET_{obs}|}{SD(ET_{obs})}$ Eq. (2)

Subscripts of 'obs' and 'mod' denote the flux observation and modeled term. The operator Σ takes the sum of the absolute difference between flux observation and model simulation output. The operator 'SD' takes the standard deviation of flux observation.

After K_{max} is optimized, we ran the model while assuming the hydraulic conductance can increase after drought. This is the simulation under the 'full recovery' assumption. However, if the model can relatively well capture the carbon and water fluxes variations over the drought period, but show overestimation after drought, such bias might be associated with a lagged response or incomplete recovery, which has not been accounted for in the 'full recovery' assumption. This model-observation gap can offer insights into the extent to which the hydraulic conductance has recovered. Such overestimation means the stress factor from model simulation is lower compared to reality, i.e. the stress itself was underestimated or the downregulation was not fully captured. Here, a realistic water stress series can be obtained by taking the observed carbon and water fluxes as constraints. This optimization was conducted per day during the post-drought period, where the simulation was iterated towards the convergence of the error function (Eq. 3). Under the no-recovery assumption, when the stress factor is applied to Vcmax, Vcmax does not recover even when water stress is relieved. However, when the stress factor is applied to g1, Vcmax is not affected, resulting in less suppression of carbon flux recovery.

For water stress series: error function =
$$\sum \frac{|GPP_{mod} - GPP_{obs}|}{SD(GPP_{obs})} + \sum \frac{|ET_{mod} - ET_{obs}|}{SD(ET_{obs})}$$
 Eq. (3)

We standardized the carbon and water fluxes from model simulation outputs by their corresponding observation values. This normalization process rendered a unit-free scalar, facilitating aggregation across various target variables. Our objective is to minimize the mean absolute standardized error of both carbon and water fluxes (Wang et al., 2021).

A schematic is shown in Figure 1. In total, the 'partial recovery scenario' falls between the 'full recovery scenario' and the 'no recovery scenario' (Figure 1c). Our model is a valuable tool for conducting sensitivity simulations to evaluate various recovery schemes related to drought legacy, with observation serving as constraints. The water stress evolution series can be disentangled to determine the extent to which the stress has been alleviated.





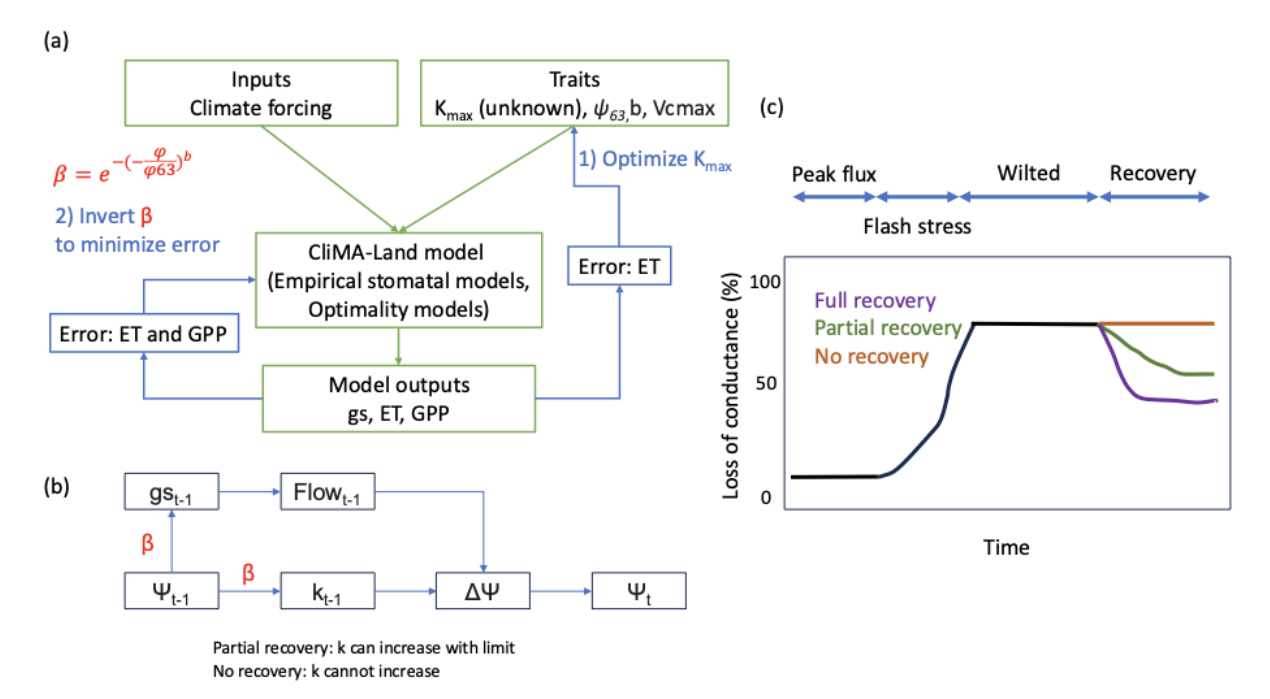


Figure 1. Schematic of the modeling framework. Abbreviations: gs, stomatal conductance; ET, evapotranspiration; GPP, gross primary productivity; φ 63: the water potential when 63% of hydraulic conductance is lost, b: shape parameter in Weibull function; Kmax, maximum hydraulic conductance. (a) Workflow of simulations and data constraints. (b) Conceptual updating of leaf water potential (φ); in empirical stomatal models, β is applied either to g1 or to Vcmax to represent water-stress effects, and β also scales hydraulic conductance ($K = Kmax \times \beta$), thereby affecting φ . (c) Time series of percentage loss of hydraulic conductance under the three recovery scenarios (full, partial, no recovery).

275 3 Results

270

280

285

3.1 2012 drought conditions

In 2012, the Central US experienced a severe drought that impacted various climatological variables, carbon and water fluxes as shown in Figure 2 for the MOFLUX site. During the earlier growing season, the air temperature exceeded records from other years, and precipitation reached the upper limit of recorded range. These conditions resulted in an overshoot (or peak flux) detected in the fluxes of GPP and ET. However, in the summer months of June and July, the monthly mean and maximum air temperature were 3 °C higher than those of other years spanning from 2007 to 2019, while summer precipitation only reached 30% of normal levels. Furthermore, the vapour pressure deficit (VPD) in July was almost double that of other years. Periodic measurements of community $\Psi_{\text{leaf,pd}}$ also showed extremely negative values as low as -4 MPa near the end of August, which was a rare occurrence. This meteorological drought led to a significant reduction in LAI, GPP, NEE and ET in the middle of 2012 (Figure 2, S1). However, in September, soil water levels began to replenish, and carbon and water fluxes gradually started to recover. While climatological stress eased at that time, fluxes only reached the lower end of the expected range from multi-year records.





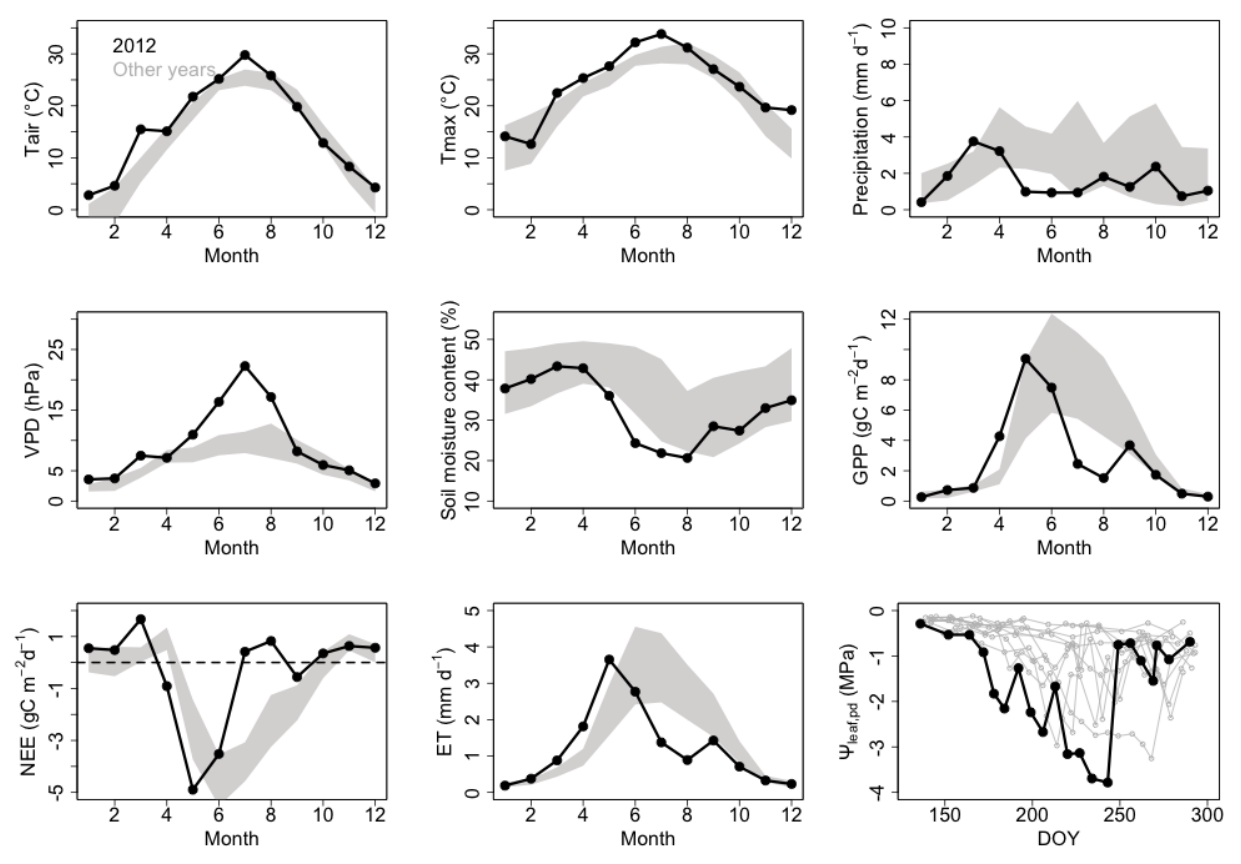


Figure 2. Drought response of meteorology, ecosystem fluxes, and plant water status. Time series of monthly mean air temperature (Tair), monthly maximum air temperature (Tmax), monthly mean precipitation rate, vapor pressure deficit (VPD), near-surface soil moisture, GPP, NEE, ET, and community predawn leaf water potential (Ψ_{leaf,pd}). The 2012 event is shown as a bold black line; the 2007–2019 record (excluding 2012) appears as gray shading indicating mean ±1σ.

3.2 Model performance

295

300

305

All tested stomatal schemes from CliMA Land demonstrated their ability to capture seasonal variations in carbon and water fluxes during the growing season of 2012 under the assumption of full recovery (Figure 3, S3). Prior to the recovery period, model simulations performed similarly (Figure 3). The performance of the optimality model and empirical stomatal models did not show distinct differences when incorporating a stress factor calculated from the loss of hydraulic conductance. Using the Medlyn stomatal model, we observed no significant differences in modeled ET between simulations where the stress factor was applied to Vcmax and g1 over the entire growing season (Wilcoxon rank test: P=0.13). However, applying the stress factor to g1 produced a higher GPP simulation compared to applying the stress factor to Vcmax (Wilcoxon rank text: P<0.001). Additionally, simulations using the stress factor on Vcmax exhibited lower RMSE for GPP at the daily scale compared to those applying the stress factor to g1 (1.40 vs. 2.67 µmol m⁻² s⁻¹).

Analyzing different time periods, GPP simulations showed higher RMSE during the recovery period compared to the peak, flash stress, and wilted periods, when the stress factor was applied to Vcmax (Figure S4). During the recovery period, applying the stress factor to g1 resulted in a larger positive bias in GPP simulations relative to observations. For ET,



320



simulations showed comparable lower biases when applying the stress factor to either Vcmax or g1 across all time periods, with no significant differences between ET simulations and flux observations over the entire growing season (Wilcoxon rank test: P>0.10).

Overall, under the full recovery assumption, model simulations tended to overestimate carbon fluxes after the drought event, especially when the stress factor was applied to g1, while accurately capturing ET dynamics (Figure 3). In contrast, under the no-recovery assumption, modeled GPP aligned more closely with observations during the recovery period when using the optimality-based stomatal model and the Medlyn-g1 setup, though ET simulations showed an underestimation (Figure 3). These comparisons between full and no-recovery scenarios highlight a lagged recovery process, underscoring the need to incorporate delayed recovery mechanisms in modeling carbon and water fluxes. Using the hydraulic trait parameters of *Acer* produced similar modeling outcomes (Figure S5), although the underestimation of photosynthesis was relatively smaller.

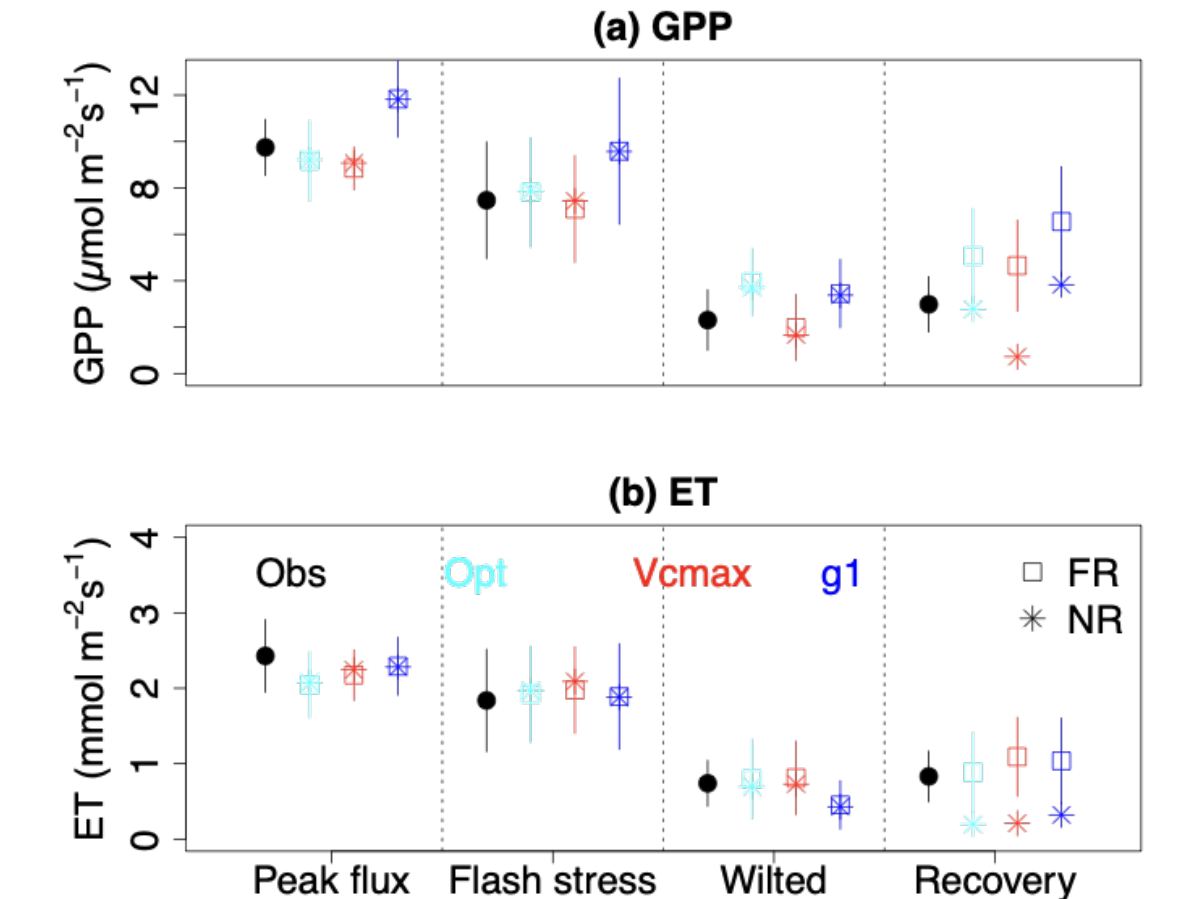


Figure 3. Model performance for GPP and ET across four periods in 2012. Curves show the optimality-based stomatal model (cyan) and the Medlyn model with the water-stress factor applied to Vcmax (red) or to g1 (blue). FR, full recovery; NR, no recovery. Error bars indicate variability within each period.



335

340

345

350

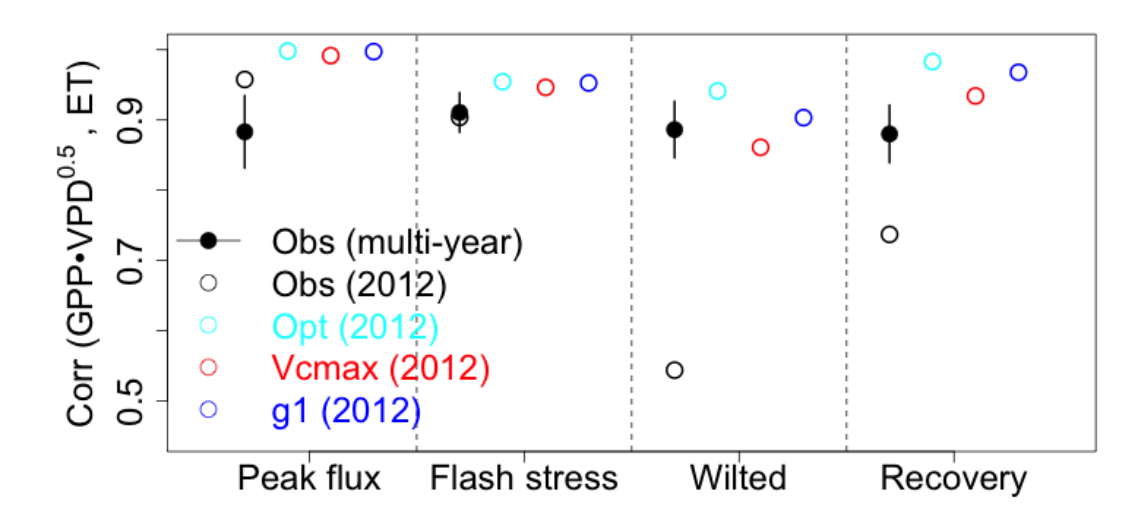


3.3 Delayed recovery of carbon fluxes

The delayed recovery of carbon fluxes relative to water fluxes suggests a lagged response driven by either stomatal or biochemical limitations. To identify the presence of non-stomatal limitations in the eddy-covariance data, we computed the daily correlation between GPP and ET (Figure 4). Our findings indicate that this correlation coefficient, representing the strength of carbon-water coupling, was relatively high during the peak flux and flash stress periods, suggesting a tightly coupled carbon and water cycle. However, during the wilted period, this correlation dropped significantly to 0.54 (compared to a multi-year average of 0.89). During the recovery period, the correlation rose to around 0.74 - higher than in the wilted period but still below the multi-year average. This suggests that non-stomatal limitations persisted into the post-drought period. Under the assumption of full recovery, model simulations overestimated the coupling strength between GPP and ET (Figure 4), further supporting the existence of lagged biochemical limitations.

Given the persistence of non-stomatal limitations after drought, we investigated whether our model could capture this lagged recovery behavior by imposing additional non-stomatal limitations. To infer the extent of partial recovery, a scenario that approximates the reality is designed by diagnostically inverting the water stress time series, using observed carbon and water fluxes as constraints when putting stress factor on either Vcmax or g1. If the stress factor on Vcmax accurately captures the lagged recovery of carbon fluxes relative to water fluxes, this would validate our findings from flux tower data. Conversely, if the stress factor on g1 performs better, it would indicate that the model incorrectly attributes the legacy effect.

After assimilating flux observations as constraints, we observed slower alleviation of water stress compared to the full recovery assumption and a similarly delayed increase in carbon fluxes. When comparing improvements in RMSE for GPP and ET between the model simulation and flux observation (shown as 'PR' relative to 'FR'), we found that incorporating lagged recovery of Vcmax enhanced model performance for both carbon and water fluxes (Figure 5). In contrast, applying the stress factor to g1 reduced RMSE for carbon fluxes but introduced a greater ET bias, revealing that this model setup fails to yield consistent improvements for both fluxes. The flux data and our modeling experiments suggest that an impairment in Vcmax delays the recovery of carbon fluxes, with the recovery process spanning days to weeks rather than occurring immediately. This finding highlights the crucial role of biochemical limitations in shaping the post-drought recovery trajectory of terrestrial ecosystems and the asymmetric recoveries of GPP and ET.



355



365

370

375

Figure 4. Carbon–water coupling strength across drought stages. Pearson correlation between daily GPP-VPD^{0.5} and ET across four periods (peak, flash-stress, wilted, recovery). Points show flux-tower observations (black) and model simulations: optimality-based stomatal model (cyan) and Medlyn with the water-stress factor applied to Vcmax (red) or g1 (blue). Correlations are computed from daily values and averaged within each period. Error bars on observations denote interannual variability; the multi-year mean is calculated over 2004–2019 excluding 2012.

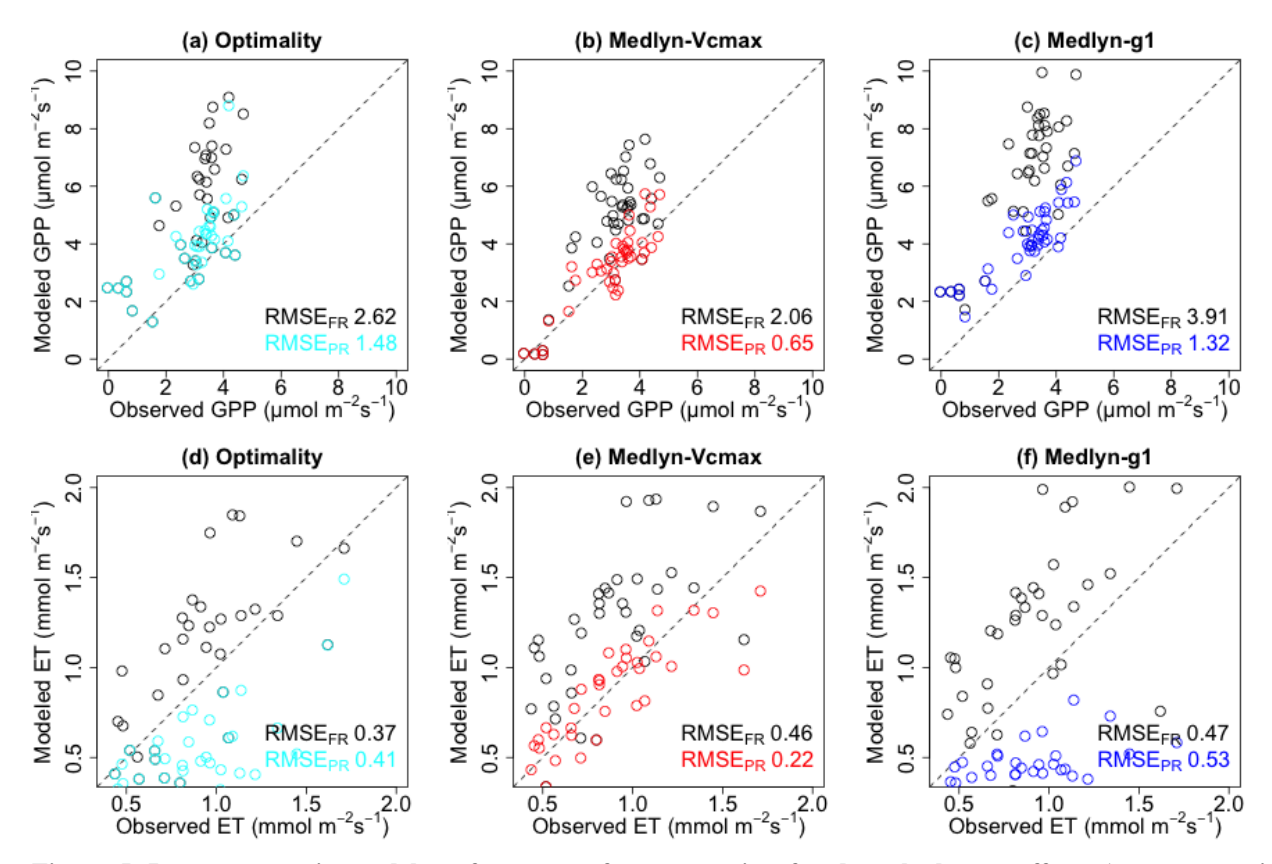


Figure 5. Improvement in model performance after accounting for drought legacy effects (recovery period only). Scatterplots compare RMSE under the partial-recovery scenario (RMSE_{PR}) against the full-recovery baseline (RMSE_{FR}) for GPP and ET. Symbols denote simulations assuming full recovery (black circles) and partial recovery using the optimality-based model (cyan) or the Medlyn model with the water-stress factor applied to Vcmax (red) or g1 (blue). RMSEs are computed against flux observations; lower values indicate better fit.

When analyzing the diurnal cycle, the model simulations successfully captured the overall shape of the diurnal changes in carbon and water fluxes (Figure 6). During the peak flux period, both carbon and water fluxes reached their maximum values at noon. As conditions transitioned into the flash stress period, the peak flux shifted earlier to around 10 am. With increasing water stress, the peak flux occurred even earlier in the morning. During the recovery periods, the diurnal shape became flatter, with the peak value returning to around noon and remaining relatively stable between 10 am and 3 pm. Under the full recovery assumption, the model predicted GPP at noon to be twice as high as observed when the stress factor was applied directly to g1, while applying the stress factor to Vcmax led to a 35% overestimation relative to observations



385

390

395

400

405



during the 10 am to 2 pm window. However, the partial recovery approach helped reduce the model-observation bias, particularly during daytime hours. Model simulations using both the optimality-based stomatal model and empirical stomatal models with the stress factor applied to Vcmax exhibited less bias across the four time periods.

It is important to note, however, that modeled peak ET around noon during the recovery periods was slightly dampened. From a modeling perspective, a decrease in Vcmax reduces carbon assimilation, which in turn suppresses stomatal conductance and transpiration. Thus, the stress applied to Vcmax effectively encompasses lumped effects from changes in Rubisco enzyme content (or activation) and environmental stress. The slightly weaker ET performance could also be due to potential shifts in the T/ET ratio between periods, highlighting the need for further exploration of inconsistent drought recovery in carbon and water fluxes. Since T/ET typically increases under dry conditions (Nie et al., 2021), we tested the model by increasing T/ET during the wilted and recovery periods and recalibrated it accordingly. This recalibration required slightly higher K_{max} values to align with the elevated T/ET during the drought. Nevertheless, this adjustment does not alter our conclusion: the delayed recovery of carbon fluxes can be effectively addressed by incorporating biochemical limitations, thereby reducing the model-observation gap.

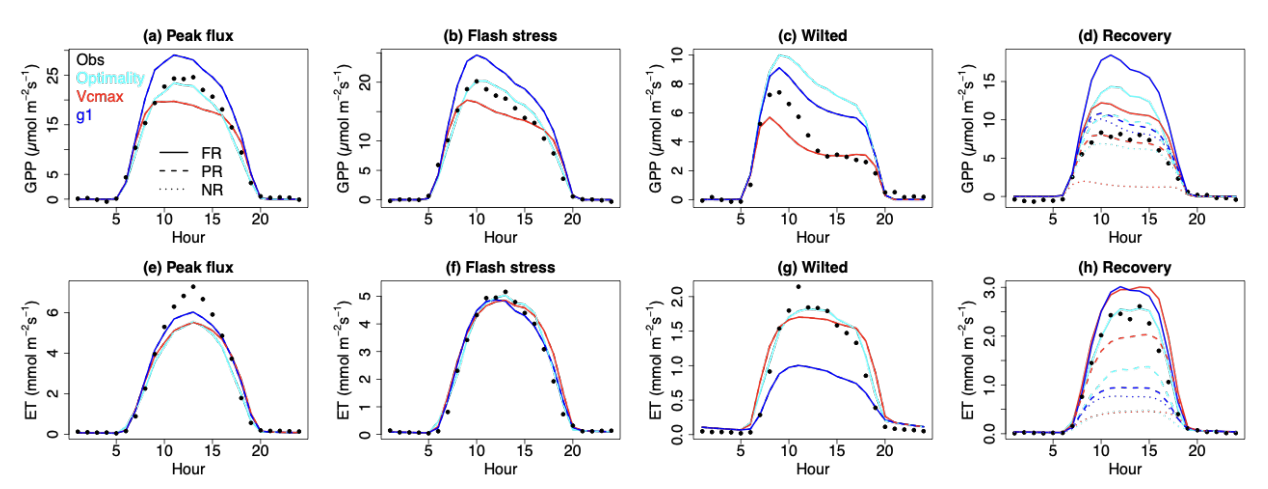


Figure 6. Diurnal cycles of GPP and ET across drought stages. Panels show (a–d) GPP and (e–h) ET for Peak flux, Flash stress, Wilted, and Recovery. Curves compare the optimality-based stomatal model (cyan) and the Medlyn model with the water-stress factor applied to Vcmax (red) or g1 (blue). Scenario keys: FR, full recovery; PR, partial recovery; NR, no recovery.

4 Discussion

This study examines the recovery of ecosystem carbon and water fluxes following the extreme drought in the Central US in 2012, using *in-situ* eddy-covariance flux measurements and the land surface model CliMA. Our findings show that CliMA accurately captured ecosystem behavior during the peak flux, flash stress, and wilted periods (Figure 3). However, during the recovery period, the model tended to overestimate carbon fluxes when assuming a complete recovery of hydraulic conductance immediately after water stress subsided. This indicates that despite the resumption of water fluxes, lingering stomatal or non-stomatal limitations may impede the recovery of carbon fluxes. Our findings align with the analysis by He et al. (He et al., 2018), which found that GPP takes longer to recover than ET. However, unlike He et al. (He



410

415

420

425

430

435

440

445



et al., 2018), who attributed the recovery of carbon and water fluxes primarily to canopy conductance, our findings indicate that introducing a progressive biochemical recovery mechanism into empirical stomatal conductance models improves model performance for both carbon and water fluxes. Specifically, we conceptualized the post-drought flux response as a composite of transient and lagged responses to environmental conditions. In this framework, the "full recovery" scenario considers only transient responses, while the "partial recovery" scenario accounts for lagged responses as well. This approach involves constructing a transient baseline for the post-drought period and quantifying deviations from the ecosystem's actual response, thereby capturing the legacy effects. Our methodology is similar to the legacy detection framework used by Yu et al. (Yu et al., 2022), which uses a machine learning model to separate transient and lagged responses, with the residuals representing the lagged component. Based on our tests of legacy detection methods, this study underscores the significance of Vcmax impairment in shaping delayed recovery of carbon fluxes. The importance of Vcmax downregulation has been noted in previous studies, such as Yang et al. (Yang et al., 2019), which demonstrated that imposing only hydraulic limitations can capture drought responses but often in a physically unrealistic manner. Other studies have also proposed adjustments to Vcmax that incorporate climate effects, yielding a better model-observation agreement (Galmés et al., 2013; Gimeno et al., 2019). Therefore, accurately modeling vegetation responses to drought requires explicitly incorporating and quantifying both stomatal and non-stomatal constraints.

While our findings highlight the significant role of lagged responses of Vcmax at the MOFLUX site, this does not imply that this phenomenon fully explains all post-drought behaviors. Model simulations at another site, US-MMS, similarly showed marked declines in both carbon and water fluxes during the drought, along with overestimations of GPP and ET in the post-drought period (Figure S6). Under the partial recovery scenario, applying the β factor to either Vcmax or g1 improved the model performance in reducing these overestimations (Figure S7). Additionally, simulations at four other sites affected by the 2012 drought successfully reproduced the seasonal dynamics of carbon and water fluxes without notable overestimations (Figure S8, S9). These results suggest that challenges remain in parametrizing stomatal and non-stomatal limitations, as the dominant limitation may vary depending on environmental conditions. The choice of whether to prioritize Vcmax or g1 should depend on the severity and duration of drought stress, underscoring the need for flexible, contextspecific modeling approaches. Short-term mild drought events may not significantly impair Rubisco activity, with stomatal closure serving as the primary limitation and non-stomatal effects playing a minor role (Wilson et al., 2000). Under prolonged drought conditions, both stomatal and non-stomatal limitations likely work together to regulate physiological responses (Galmés et al., 2007). For example, observations at the MOFLUX site revealed carbon-water decoupling during drought and recovery periods, implying the important role of biochemical limitations in regulating these processes. Stomatal limitations are observed across a wide range of soil moisture levels, while non-stomatal limitations become more prominent under moderate to extreme water deficits (Drake et al., 2017). Reductions in the stomatal slope parameter often precede reductions in Vcmax, although Rubisco content may increase under prolonged drought due to acclimation (Zhou et al., 2018). Similarly, Flexas et al. (Flexas et al., 2006) noted a strong connection between stomatal conductance and Vcmax, with Rubisco activity declining only when stomatal conductance drops below a critical threshold. The transition between these two types of limitations could depend on factors such as leaf position and water content (Song et al., 2020), while Drake et al. (Drake et al., 2017) argued that these limitations often act concurrently rather than in distinct phases. As decreased Rubisco activity can hinder rapid recovery even after rehydration (Varone et al., 2012), understanding the thresholds beyond which non-stomatal limitations dominate requires further sensitivity experiments to mechanistically unravel the interconnected dynamics of carbon and water fluxes during recovery from extreme climate events.

Although the model simulation in this study parameterized a single set of plant hydraulics parameters based on the site's dominant tree species of oak, known for its drought-resistant characteristics, we recognize that drought responses can vary significantly among tree species with diverse hydraulic regulation strategies (Drake et al., 2017; Zhou et al., 2014). For



460

465

470

485

490



instance, Rehschuh and Ruehr (Rehschuh and Ruehr, 2022) observed no necessary connection between hydraulic impairment and lagged photosynthetic recovery in Scots pine. Xeric tree species, on the other hand, tend to experience more negative leaf water potentials at which photosynthetic efficiency declines sharply (Zhou et al., 2014). Species-specific differences also emerge in the relative contributions of stomatal and biochemical limitations (Zhou et al., 2015). These findings underscore the need to extend our analysis framework to encompass a broader range of tree species, considering variations in life stage, the drought timing, intensity, and duration of stress period, as well as species-specific resistance and resilience to drought.

Our findings emphasize the significance of accounting for drought-induced damage to Vcmax and its subsequent delayed impacts on carbon and water fluxes. This study represents a preliminary application of our modeling framework at a representative eddy-covariance site impacted by the 2012 mega drought, aimed at identifying lagged responses in carbon and water flux as well as stomatal and non-stomatal limitations. Our analysis revealed that, beyond the transient responses of carbon flux, a lagged biochemical recovery helps bridge the model-observation gap. This site-level research lays the groundwork for potential regional expansions to delve further into the factors influencing drought recovery and to validate the generalizability of the identified responses. To enhance predictions of ecosystem resilience to future climate challenges, further studies should evaluate the asynchronous responses of biochemical and stomatal limitations to drought and explore their underlying drivers. A critical implication of our research is that most current Earth system models lack the inclusion of this vital mechanism. As a result, their projections of carbon sequestration may be overly optimistic, raising concerns about the reliability of these models in informing mitigation policies. By incorporating these crucial processes into Earth system models, we can develop more reliable projections and help make informed decisions to effectively address the climate change challenges. Additionally, considering the potential asynchronous recovery rates of carbon and water fluxes will provide valuable insights into the possible carbon-water decoupling behavior during extreme events (De Kauwe et al., 2019; Krich et al., 2022).

To reduce the long-term impacts of drought legacy effects on forest ecosystems, management strategies should focus on enhancing resilience and adaptive capacity. Selective thinning can lessen competition for water, enabling surviving trees to recover more effectively after drought. Increasing species diversity—particularly through the inclusion of drought-tolerant and deep-rooted species—can help buffer stands against future water stress. Regular monitoring of physiological indicators, such as canopy water content and stomatal conductance, can reveal delayed drought responses and guide timely interventions. Integrating drought legacy effects into forest growth models will be critical for sustaining carbon sequestration and maintaining ecosystem services under a changing climate.

5 Conclusion

In this study, we conducted a comprehensive investigation of the drought response during the 2012 drought in the Central US, utilizing *in-situ* eddy-covariance flux measurements and the CliMA model. Observations revealed a quick resumption of ET but a slower recovery of carbon fluxes. Our drought response simulations showed that assuming full recovery of hydraulic conductance leads to an overestimation of carbon flux recovery. To address this limitation, we introduced a progressive biochemical recovery process into the model diagnostically, accounting for the impairment of Rubisco activity. This modification led to enhanced model performance in simulating both carbon and water fluxes, offering more accurate representation of the ecosystem's recovery dynamics. The implications of this finding are particularly relevant in the context of increasing frequency and intensity of extreme climate events. Ignoring legacy effects and relying on overly





optimistic estimations of future land carbon uptake could be misleading, emphasizing the need for more in-depth studies on understanding ecosystem resilience to extreme climate events.

495

Data availability

Ecosystem flux data for US-MOz is downloaded from https://ameriflux.lbl.gov. Predawn leaf water potential measurement at Ozark site can be downloaded from https://data.ess-dive.lbl.gov/view/doi:10.3334/CDIAC/ORNLSFA.004

500 Code availability

CliMA Land model code can be accessed at https://github.com/CliMA/Land

Author contributions

YY and YW conceived the initial idea. YY performed the analysis, conducted the model experiments and wrote the manuscript. All authors read and approved the final manuscript.

505 Declaration of competing interest

The authors declare that they have no conflict of interest.

Acknowledgement

This work was funded by the NASA Carbon Cycle Science Program (80NSSC21K1712).

References

- Anderegg, W. R. L., Schwalm, C., Biondi, F., Camarero, J. J., Koch, G., Litvak, M., Ogle, K., Shaw, J. D., Shevliakova, E., Williams, A. P., Wolf, A., Ziaco, E., and Pacala, S.: FOREST ECOLOGY. Pervasive drought legacies in forest ecosystems and their implications for carbon cycle models, Science, 349, 528–532, 2015.
- Ball, J. T., Woodrow, I. E., and Berry, J. A.: A model predicting stomatal conductance and its contribution to the control of photosynthesis under different environmental conditions, in: Progress in Photosynthesis Research, Springer Netherlands,
 Dordrecht, 221–224, 1987.
 - Basara, J. B., Christian, J. I., Wakefield, R. A., Otkin, J. A., Hunt, E. H., and Brown, D. P.: The evolution, propagation, and spread of flash drought in the Central United States during 2012, Environ. Res. Lett., 14, 084025, 2019.
 - Bastos, A., Ciais, P., Friedlingstein, P., Sitch, S., Pongratz, J., Fan, L., Wigneron, J. P., Weber, U., Reichstein, M., Fu, Z., Anthoni, P., Arneth, A., Haverd, V., Jain, A. K., Joetzjer, E., Knauer, J., Lienert, S., Loughran, T., McGuire, P. C., Tian, H.,





- Viovy, N., and Zaehle, S.: Direct and seasonal legacy effects of the 2018 heat wave and drought on European ecosystem productivity, Sci. Adv., 6, eaba2724, 2020.
 - Benson, M. C., Miniat, C. F., Oishi, A. C., Denham, S. O., Domec, J.-C., Johnson, D. M., Missik, J. E., Phillips, R. P., Wood, J. D., and Novick, K. A.: The xylem of anisohydric Quercus alba L. is more vulnerable to embolism than isohydric codominants, Plant Cell Environ., 45, 329–346, 2022.
- Braghiere, R. K., Wang, Y., Doughty, R., Sousa, D., Magney, T., Widlowski, J.-L., Longo, M., Bloom, A. A., Worden, J., Gentine, P., and Frankenberg, C.: Accounting for canopy structure improves hyperspectral radiative transfer and sun-induced chlorophyll fluorescence representations in a new generation Earth System model, Remote Sens. Environ., 261, 112497, 2021.
- Ciais, P., Reichstein, M., Viovy, N., Granier, A., Ogée, J., Allard, V., Aubinet, M., Buchmann, N., Bernhofer, C., Carrara,
 A., Chevallier, F., De Noblet, N., Friend, A. D., Friedlingstein, P., Grünwald, T., Heinesch, B., Keronen, P., Knohl, A., Krinner, G., Loustau, D., Manca, G., Matteucci, G., Miglietta, F., Ourcival, J. M., Papale, D., Pilegaard, K., Rambal, S., Seufert, G., Soussana, J. F., Sanz, M. J., Schulze, E. D., Vesala, T., and Valentini, R.: Europe-wide reduction in primary productivity caused by the heat and drought in 2003, Nature, 437, 529–533, 2005.
- De Kauwe, M. G., Kala, J., Lin, Y.-S., Pitman, A. J., Medlyn, B. E., Duursma, R. A., Abramowitz, G., Wang, Y.-P., and Miralles, D. G.: A test of an optimal stomatal conductance scheme within the CABLE land surface model, Geosci. Model Dev., 8, 431–452, 2015.
 - De Kauwe, M. G., Medlyn, B. E., Pitman, A. J., Drake, J. E., Ukkola, A., Griebel, A., Pendall, E., Prober, S., and Roderick, M.: Examining the evidence for decoupling between photosynthesis and transpiration during heat extremes, Biogeosciences, 16, 903–916, 2019.
- Drake, J. E., Power, S. A., Duursma, R. A., Medlyn, B. E., Aspinwall, M. J., Choat, B., Creek, D., Eamus, D., Maier, C., Pfautsch, S., Smith, R. A., Tjoelker, M. G., and Tissue, D. T.: Stomatal and non-stomatal limitations of photosynthesis for four tree species under drought: A comparison of model formulations, Agric. For. Meteorol., 247, 454–466, 2017.
 - Duursma, R. A.: Plantecophys--an R package for analysing and modelling leaf gas exchange data, PLoS One, 10, e0143346, 2015.
- Egea, G., Verhoef, A., and Vidale, P. L.: Towards an improved and more flexible representation of water stress in coupled photosynthesis-stomatal conductance models, Agric. For. Meteorol., 151, 1370–1384, 2011.
 - Eller, C. B., Rowland, L., Mencuccini, M., Rosas, T., Williams, K., Harper, A., Medlyn, B. E., Wagner, Y., Klein, T.,



570



Teodoro, G. S., Oliveira, R. S., Matos, I. S., Rosado, B. H. P., Fuchs, K., Wohlfahrt, G., Montagnani, L., Meir, P., Sitch, S., and Cox, P. M.: Stomatal optimization based on xylem hydraulics (SOX) improves land surface model simulation of vegetation responses to climate, New Phytol., 226, 1622–1637, 2020.

Fang, J. and Gentine, P.: Exploring optimal complexity for water stress representation in terrestrial carbon models: A hybrid-machine learning model approach, J. Adv. Model. Earth Syst., 16, https://doi.org/10.1029/2024ms004308, 2024.

Farquhar, G. D., von Caemmerer, S., and Berry, J. A.: A biochemical model of photosynthetic CO2 assimilation in leaves of C 3 species, Planta, 149, 78–90, 1980.

Fatichi, S. and Pappas, C.: Constrained variability of modeled *T:ET* ratio across biomes: Transpiration:Evapotranspiration Ratio, Geophys. Res. Lett., 44, 6795–6803, 2017.

Flexas, J., Ribas-Carbó, M., Bota, J., Galmés, J., Henkle, M., Martínez-Cañellas, S., and Medrano, H.: Decreased Rubisco activity during water stress is not induced by decreased relative water content but related to conditions of low stomatal conductance and chloroplast CO2 concentration, New Phytol., 172, 73–82, 2006.

560 Galmés, J., Medrano, H., and Flexas, J.: Photosynthetic limitations in response to water stress and recovery in Mediterranean plants with different growth forms, New Phytol., 175, 81–93, 2007.

Galmés, J., Aranjuelo, I., Medrano, H., and Flexas, J.: Variation in Rubisco content and activity under variable climatic factors, Photosynth. Res., 117, 73–90, 2013.

Gimeno, T. E., Saavedra, N., Ogée, J., Medlyn, B. E., and Wingate, L.: A novel optimization approach incorporating nonstomatal limitations predicts stomatal behaviour in species from six plant functional types, J. Exp. Bot., 70, 1639–1651, 2019.

Gourlez de la Motte, L., Beauclaire, Q., Heinesch, B., Cuntz, M., Foltýnová, L., Šigut, L., Kowalska, N., Manca, G., Ballarin, I. G., Vincke, C., Roland, M., Ibrom, A., Lousteau, D., Siebicke, L., Neiryink, J., and Longdoz, B.: Non-stomatal processes reduce gross primary productivity in temperate forest ecosystems during severe edaphic drought, Philos. Trans. R. Soc. Lond. B Biol. Sci., 375, 20190527, 2020.

Gu, L., Pallardy, S. G., Tu, K., Law, B. E., and Wullschleger, S. D.: Reliable estimation of biochemical parameters from C₃ leaf photosynthesis-intercellular carbon dioxide response curves: Estimating FvCB model parameters, Plant Cell Environ., 33, 1852–1874, 2010.

Gu, L., Pallardy, S. G., Hosman, K. P., and Sun, Y.: Drought-influenced mortality of tree species with different predawn leaf





- water dynamics in a decade-long study of a central US forest, Biogeosciences, 12, 2831–2845, 2015.
 - Gu, L., Pallardy, S. G., Yang, B., Hosman, K. P., Mao, J., Ricciuto, D., Shi, X., and Sun, Y.: Testing a land model in ecosystem functional space via a comparison of observed and modeled ecosystem flux responses to precipitation regimes and associated stresses in a Central U.S. forest: Test Model in Ecosystem Functional Space, J. Geophys. Res. Biogeosci., 121, 1884–1902, 2016.
- He, B., Liu, J., Guo, L., Wu, X., Xie, X., Zhang, Y., Chen, C., Zhong, Z., and Chen, Z.: Recovery of ecosystem carbon and energy fluxes from the 2003 drought in Europe and the 2012 drought in the United States, Geophys. Res. Lett., 45, 4879–4888, 2018.
 - Kannenberg, S. A., Schwalm, C. R., and Anderegg, W. R. L.: Ghosts of the past: how drought legacy effects shape forest functioning and carbon cycling, Ecol. Lett., 23, 891–901, 2020.
- Keenan, T., García, R., Friend, A. D., Zaehle, S., Gracia, C., and Sabate, S.: Improved understanding of drought controls on seasonal variation in Mediterranean forest canopy CO₂ and water fluxes through combined in situ measurements and ecosystem modelling, Biogeosciences, 6, 1423–1444, 2009.
- Keenan, T., Sabate, S., and Gracia, C.: Soil water stress and coupled photosynthesis—conductance models: Bridging the gap between conflicting reports on the relative roles of stomatal, mesophyll conductance and biochemical limitations to photosynthesis, Agric. For. Meteorol., 150, 443–453, 2010.
 - Kennedy, D., Swenson, S., Oleson, K. W., Lawrence, D. M., Fisher, R., da Costa, A. C. L., and Gentine, P.: Implementing Plant Hydraulics in the Community Land Model, Version 5, Journal of Advances in Modeling Earth Systems, 11, 485–513, 2019.
- Krich, C., Mahecha, M. D., Migliavacca, M., De Kauwe, M. G., Griebel, A., Runge, J., and Miralles, D. G.: Decoupling between ecosystem photosynthesis and transpiration: a last resort against overheating, Environ. Res. Lett., 17, 044013, 2022.
 - Leuning, R.: A critical appraisal of a combined stomatal-photosynthesis model for C₃ plants, Plant Cell Environ., 18, 339–355, 1995.
- Medlyn, B. E., Duursma, R. A., Eamus, D., Ellsworth, D. S., Prentice, I. C., Barton, C. V. M., Crous, K. Y., de Angelis, P.,
 Freeman, M., and Wingate, L.: Reconciling the optimal and empirical approaches to modelling stomatal conductance:
 RECONCILING OPTIMAL AND EMPIRICAL STOMATAL MODELS, Glob. Chang. Biol., 17, 2134–2144, 2011.
 - Müller, L. M. and Bahn, M.: Drought legacies and ecosystem responses to subsequent drought, Glob. Chang. Biol., 28,



625



5086-5103, 2022.

Neufeld, H. S., Grantz, D. A., Meinzer, F. C., Goldstein, G., Crisosto, G. M., and Crisosto, C.: Genotypic variability in vulnerability of leaf xylem to cavitation in water-stressed and well-irrigated sugarcane, Plant Physiol., 100, 1020–1028, 1992.

Nie, C., Huang, Y., Zhang, S., Yang, Y., Zhou, S., Lin, C., and Wang, G.: Effects of soil water content on forest ecosystem water use efficiency through changes in transpiration/evapotranspiration ratio, Agric. For. Meteorol., 308-309, 108605, 2021.

Niinemets, Ü. and Keenan, T.: Photosynthetic responses to stress in Mediterranean evergreens: Mechanisms and models, Environ. Exp. Bot., 103, 24–41, 2014.

Piao, S., Zhang, X., Chen, A., Liu, Q., Lian, X., Wang, X., Peng, S., and Wu, X.: The impacts of climate extremes on the terrestrial carbon cycle: A review, Sci. China Earth Sci., 62, 1551–1563, 2019.

Rehschuh, R. and Ruehr, N. K.: Diverging responses of water and carbon relations during and after heat and hot drought stress in Pinus sylvestris, Tree Physiol., 42, 1532–1548, 2022.

Reichstein, M., Tenhunen, J., Roupsard, O., Ourcival, J.-M., Rambal, S., Miglietta, F., Peressotti, A., Pecchiari, M., Tirone, G., and Valentini, R.: Inverse modeling of seasonal drought effects on canopy CO₂/H₂O exchange in three Mediterranean ecosystems, J. Geophys. Res., 108, https://doi.org/10.1029/2003jd003430, 2003.

Song, X., Zhou, G., He, Q., and Zhou, H.: Stomatal limitations to photosynthesis and their critical Water conditions in different growth stages of maize under water stress, Agric. Water Manag., 241, 106330, 2020.

Sperry, J. S., Venturas, M. D., Anderegg, W. R. L., Mencuccini, M., Mackay, D. S., Wang, Y., and Love, D. M.: Predicting stomatal responses to the environment from the optimization of photosynthetic gain and hydraulic cost, Plant Cell Environ., 40, 816–830, 2017.

Varone, L., Ribas-Carbo, M., Cardona, C., Gallé, A., Medrano, H., Gratani, L., and Flexas, J.: Stomatal and non-stomatal limitations to photosynthesis in seedlings and saplings of Mediterranean species pre-conditioned and aged in nurseries: Different response to water stress, Environ. Exp. Bot., 75, 235–247, 2012.

Wang, Y. and Frankenberg, C.: On the impact of canopy model complexity on simulated carbon, water, and solar-induced chlorophyll fluorescence fluxes, Biogeosciences, 19, 29–45, 2022.

Wang, Y., Sperry, J. S., Anderegg, W. R. L., Venturas, M. D., and Trugman, A. T.: A theoretical and empirical assessment





of stomatal optimization modeling, New Phytol., 227, 311-325, 2020.

- Wang, Y., Köhler, P., He, L., Doughty, R., Braghiere, R. K., Wood, J. D., and Frankenberg, C.: Testing stomatal models at the stand level in deciduous angiosperm and evergreen gymnosperm forests using CliMA Land (v0.1), Geosci. Model Dev., 14, 6741–6763, 2021.
 - Wang, Y., Köhler, P., Braghiere, R. K., Longo, M., Doughty, R., Bloom, A. A., and Frankenberg, C.: GriddingMachine, a database and software for Earth system modeling at global and regional scales, Sci. Data, 9, 258, 2022.
- Wang, Y., Braghiere, R. K., Longo, M., Norton, A. J., Köhler, P., Doughty, R., Yin, Y., Bloom, A. A., and Frankenberg, C.: Modeling global vegetation gross primary productivity, transpiration and hyperspectral canopy radiative transfer simultaneously using a next generation land surface model—CliMA land, J. Adv. Model. Earth Syst., 15, https://doi.org/10.1029/2021ms002964, 2023.
- Wilson, K. B., Baldocchi, D. D., and Hanson, P. J.: Quantifying stomatal and non-stomatal limitations to carbon assimilation resulting from leaf aging and drought in mature deciduous tree species, Tree Physiol., 20, 787–797, 2000.
 - Wolf, A., Akshalov, K., Saliendra, N., Johnson, D. A., and Laca, E. A.: Inverse estimation of Vc_{max}, leaf area index, and the Ball-Berry parameter from carbon and energy fluxes, J. Geophys. Res., 111, https://doi.org/10.1029/2005jd005927, 2006.
- Wolf, S., Keenan, T. F., Fisher, J. B., Baldocchi, D. D., Desai, A. R., Richardson, A. D., Scott, R. L., Law, B. E., Litvak, M. E., Brunsell, N. A., Peters, W., and van der Laan-Luijkx, I. T.: Warm spring reduced carbon cycle impact of the 2012 US summer drought, Proc. Natl. Acad. Sci. U. S. A., 113, 5880–5885, 2016.
 - Wood, J. D., Gu, L., Hanson, P. J., Frankenberg, C., and Sack, L.: The ecosystem wilting point defines drought response and recovery of a Quercus-Carya forest, Glob. Chang. Biol., 29, 2015–2029, 2023.
- Wu, X., Liu, H., Li, X., Ciais, P., Babst, F., Guo, W., Zhang, C., Magliulo, V., Pavelka, M., Liu, S., Huang, Y., Wang, P., Shi, C., and Ma, Y.: Differentiating drought legacy effects on vegetation growth over the temperate Northern Hemisphere, Glob. Chang. Biol., 24, 504–516, 2018.
 - Xu, C., McDowell, N. G., Fisher, R. A., Wei, L., Sevanto, S., Christoffersen, B. O., Weng, E., and Middleton, R. S.: Increasing impacts of extreme droughts on vegetation productivity under climate change, Nat. Clim. Chang., 9, 948–953, 2019.
- Xu, X., Medvigy, D., Powers, J. S., Becknell, J. M., and Guan, K.: Diversity in plant hydraulic traits explains seasonal and inter-annual variations of vegetation dynamics in seasonally dry tropical forests, New Phytol., 212, 80–95, 2016.





Yang, J., Duursma, R. A., De Kauwe, M. G., Kumarathunge, D., Jiang, M., Mahmud, K., Gimeno, T. E., Crous, K. Y., Ellsworth, D. S., Peters, J., Choat, B., Eamus, D., and Medlyn, B. E.: Incorporating non-stomatal limitation improves the performance of leaf and canopy models at high vapour pressure deficit, Tree Physiol., 39, 1961–1974, 2019.

Yao, Y., Joetzjer, E., Ciais, P., Viovy, N., Cresto Aleina, F., Chave, J., Sack, L., Bartlett, M., Meir, P., Fisher, R., and Luyssaert, S.: Forest fluxes and mortality response to drought: model description (ORCHIDEE-CAN-NHA r7236) and evaluation at the Caxiuanã drought experiment, Geosci. Model Dev., 15, 7809–7833, 2022.

Yuan, H., Dai, Y., Xiao, Z., Ji, D., and Shangguan, W.: Reprocessing the MODIS Leaf Area Index products for land surface and climate modelling, Remote Sens. Environ., 115, 1171–1187, 2011.

Yu, X., Orth, R., Reichstein, M., Bahn, M., Klosterhalfen, A., Knohl, A., Koebsch, F., Migliavacca, M., Mund, M., Nelson,
 J. A., Stocker, B. D., Walther, S., and Bastos, A.: Contrasting drought legacy effects on gross primary productivity in a mixed versus pure beech forest, Biogeosciences, 19, 4315–4329, 2022.

Zhao, K., Ryu, Y., Hu, T., Garcia, M., Li, Y., Liu, Z., Londo, A., and Wang, C.: How to better estimate leaf area index and leaf angle distribution from digital hemispherical photography? Switching to a binary nonlinear regression paradigm, Methods Ecol. Evol., 10, 1864–1874, 2019.

Zhou, L., Wang, S., Chi, Y., Li, Q., Huang, K., and Yu, Q.: Responses of photosynthetic parameters to drought in subtropical forest ecosystem of China, Sci. Rep., 5, 18254, 2015.

Zhou, S., Duursma, R. A., Medlyn, B. E., Kelly, J. W. G., and Prentice, I. C.: How should we model plant responses to drought? An analysis of stomatal and non-stomatal responses to water stress, Agric. For. Meteorol., 182-183, 204–214, 2013.

Zhou, S., Medlyn, B., Sabaté, S., Sperlich, D., and Prentice, I. C.: Short-term water stress impacts on stomatal, mesophyll and biochemical limitations to photosynthesis differ consistently among tree species from contrasting climates, Tree Physiol., 34, 1035–1046, 2014.

Zhou, S.-X., Prentice, I. C., and Medlyn, B. E.: Bridging drought experiment and modeling: Representing the differential sensitivities of leaf gas exchange to drought, Front. Plant Sci., 9, 1965, 2018.

680